Rapid Non-Contact Optical Ultrasound for Biomedical Imaging

Erwin J Alles*,†
*Wellcome / EPSRC Centre for Interventional and Surgical Sciences, University College London, London, UK
†Department of Medical Physics & Biomedical Engineering, University College London, London, UK

2023 IEEE International Ultrasonics Symposium (IUS) | 979-8-3503-4645-9/23/$31.00 ©2023 IEEE | DOI: 10.1109/IUS51837.2023.10306919

***Abstract*—Biomedical ultrasound imaging is typically performed using electronic transducer technology, which results in imaging probes exhibiting large mechanical footprints that require physical contact with the imaging target. While this mature technology allows for high-quality, versatile free-hand imaging, its applicability is limited in crowded surgical settings and scenarios at risk of infection or trauma. Instead, here a novel system is presented that enables non-contact ultrasound imaging through remote sensing. This is achieved using light rather than electronics to both generate and detect ultrasound, which is delivered in free-space to the surface of the object by weakly-focussed beams. To maximise the signal fidelity, a custom membrane was developed that is deposited to the surface of the imaging target. The combined system and membrane currently achieve real-time and dynamic imaging at a frame rate of up to 22 Hz for highly reflective targets, and requires an acquisition time of *ca.* 27 s for physiologically relevant phantoms. As such, the system already achieves clinically relevant performance for, e.g., needle or instrument tracking, and various improvements are suggested that in the near future will significantly accelerate image acquisition of soft tissue – ultimately resulting in sub-second biomedical non-contact ultrasound imaging.**

***Index Terms*—Non-contact ultrasound, optical ultrasound, skin-applied ultrasound generating membrane, laser Doppler vibrometer**

I. Introduction

Biomedical ultrasound is conventionally performed using imaging probes comprising electronic transducers, which enable versatile and freehand imaging, in real-time and at video-rate [1]. However, such electronic imaging probes require physical contact to ensure good acoustic coupling, and the piezoelectric transducers, front-end electronics and cabling result in a large footprint – thus prohibiting applications in crowded surgical settings (such as robot-assisted surgery) or in scenarios at risk of trauma or infection (such as wounds and intra-operative imaging).

Inspired by approaches taken for non-destructive testing, where non-contact laser ultrasound inspection is routinely performed [2], the first biomedical non-contact optical ultrasound (NC-OpUS) imaging was recently demonstrated in bench top [3] and first-on-human settings [4]. Here, pulsed laser light was photoacoustically (PA) converted into ultrasound at the tissue surface, thus emitting an ultrasound wave that propagates into the surrounding tissue. Back-scattered ("pulse-echo") waves result in minute deformations of the tissue surface that are detected interferometrically using, e.g., a laser Doppler vibrometer (LDV) [5]. While both systems enabled ultrasound imaging in absence of physical contact, 2D image acquisition times were in the order of minutes due to a low PA conversion efficiency, low LDV signal-to-noise ratio (SNR), and low laser pulse repetition rates.

Here, a novel NC-OpUS system is presented that follows a similar approach, but includes a number of important innovations: the system uses a high-repetition-rate laser combined with fast scanning optics; parallel data acquisition, reconstruction and display; and optimized aperture geometries. Importantly, a custom NC-OpUS membrane was developed, combined with a method of applying this to human skin, that simultaneously maximises PA conversion efficiency and LDV SNR – ultimately resulting in a system capable of real-time, dynamic imaging.

II. Methods

A. Experimental setup

Light from a fast pulsed laser (wavelength: 532 nm, pulse duration: 2 ns, pulse energy: 29 μJ, pulse repetition rate: 2.5 kHz; FDSS532-Q3, Crylas, Germany) was incident on a set of scanning mirrors (GVS002, Thorlabs, Germany) controlled by an I/O device (NI USB-6211, National Instruments Corp., TX, USA), and focussed (focal length: 150 mm; LA1433-A, Thorlabs, Germany) onto a custom membrane. This membrane was placed at the air-water interface of a water bath, which was located approximately 28 cm from the scanning mirror.

The resulting ultrasound waves propagated into the water bath, back-scattered off sample inhomogeneities, and caused deformations in the membrane. These deformations were detected using a broadband LDV (bandwidth: $0 - 12$ MHz; VibroFlex Neo [VFX-I-110] + Connect [VFX-F-110] + short range lens [VFX-O-SRS], Polytec, Germany), and the detected signals were recorded by a high-speed digitiser (sample rate: 250 MSa/s, bit depth: 16 bits; M4i.4420-x8, Spectrum, Germany).

A custom LabVIEW (National Instruments Corp., TX, USA) script was used to control all the equipment, synchronise laser triggering, and perform real-time data acquisition, signal processing, image reconstruction, and visualisation. The experimental setup is depicted in Fig. 1.

This work was supported by the Wellcome/EPSRC Centre for Interventional and Surgical Sciences (WEISS) (203145Z/16/Z), the Rosetrees Trust (PGS19-2/10006), and the Academy of Medical Sciences (SBF007/100006). The author gratefully acknowledges the support of the NVIDIA Corporation through the donation of the Quadro P6000 GPU used for this research, and of Dr Efthymios Maneas for providing the tissue-mimicking phantom.

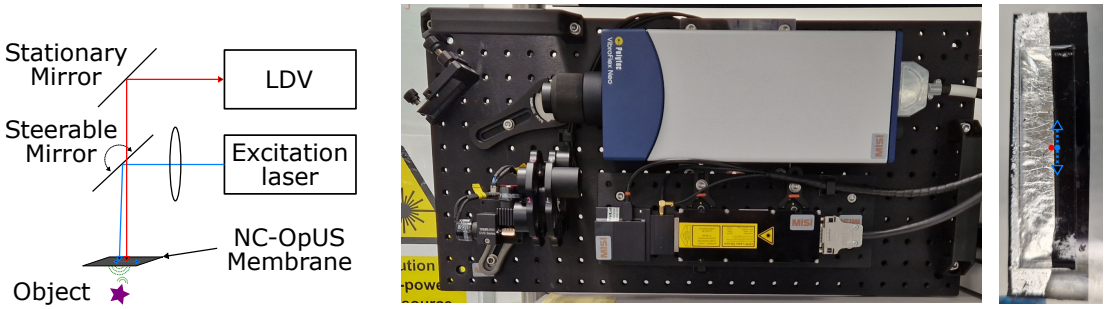

Fig. 1. **The experimental NC-OpUS setup. (a)** Schematic of the experimental setup. **(b)** Corresponding photograph of the setup, which is mounted vertically. The object and water bath are not shown. **(c)** Photograph of the custom NC-OpUS membrane. The left half is reflective to optimize detection SNR; the right half is optically absorbing to optimize the photoacoustic conversion efficiency. Approximate locations of the stationary LDV detection spot (red) and the scanned excitation spot and imaging aperture (blue) are indicated. This membrane was stretched across an acrylic frame to facilitate level mounting.

B. Signal acquisition and processing

The use of scanning optics allowed for arbitrary control over the positioning of the excitation light. This enabled the synthesis of imaging apertures of arbitrary size and geometry, comprising arbitrary numbers of sources. In this study, aperture geometries were limited to 1D to achieve 2D NC-OpUS imaging, however the two-axis set of scanning mirrors used in principle allows for 2D imaging apertures to achieve 3D imaging.

The sources were either uniformly distributed across the aperture, or spatial source density apodization (SDA) was applied [6] to suppress side and grating lobes, and additional Hamming amplitude apodization was applied to further suppress side lobes. To avoid membrane burn-in, signal averaging was performed (where applicable) through repeatedly scanning the entire source aperture rather than repeating the same source position.

The LDV was configured to apply a 12 MHz low-pass filter, and recorded pulse-echo data were reconstructed into images using a basic delay-and-sum algorithm [7], which was GPU-accelerated (Quadro P6000, Nvidia, CA, USA) using the Nvidia CUDA toolbox (v11.7). To improve imaging frame rate, data acquisition and signal processing for the current frame were performed in parallel with the image reconstruction of the previous frame.

C. Membrane fabrication

To simultaneously improves the PA conversion efficiency and LDV SNR, a custom membrane was developed that was deposited on the surface of the imaging scenario. This membrane comprised a composite of an elastomeric host (polydimethylsiloxane; MED-1000, Nu-Sil, CA, USA) and optically absorbing mesoporous carbon powder (1.6%-wt; SKU 699632, Sigma-Aldrich, MO, USA), which was diluted with Neo-Clear (31.7%-vol; SKU 1098435000, Sigma-Aldrich, MO, USA) to facilitate handling and reduce membrane thickness upon evaporation during curing. Doctor blading was applied to fabricate membranes, at ambient conditions, with a thickness of 25 µm, an -6 dB acoustic bandwidth ranging from 8 to 38 MHz, an optical absorption coefficient $>$ 98% at the excitation wavelength, and a PA conversion efficiency of 0.034 MPa/(mJ/cm^2).

The PA conversion efficiency achieved is comparable to some of the highest values reported in literature [8]. However, the mesoporous carbon used here instead of common alternatives avoided the inherent variability observed during open flame deposition of candle soot [8] by using a commercially available alternative, and removed health risks and stigmas associated with the use of nanoparticles such as carbon nanotubes [9]. In addition, the use of Neo-Clear instead of the commonly used xylenes obviated the need for sample preparation to take place inside a fume hood, and its reduced flammability facilitated its handling.

Part of the membrane was engineered to be reflective to improve the LDV SNR. This was achieved by embedding a silver foil (thickness: $<$ 1 µm; Fuyoal, China) in the membrane to act as a mirror, and the LDV light was focused onto this reflective section at normal incidence. One such membrane comprising both a reflective and optically absorbing region is shown in Fig. 1(c).

D. Imaging scenarios

Two imaging phantoms were used to assess the performance of the system. First, a highly echogenic steel wire (diameter: 0.8 mm) placed orthogonal to the imaging plane was used to assess the imaging resolution, contrast, and maximum frame rate. No averaging was performed for this phantom, and the source aperture comprised 64 sources distributed across a 6.0 mm-wide aperture following a "circular" SDA geometry [6] to suppress grating lobes. For this SDA geometry, the number of sources per unit distance across the aperture were stipulated by the circle equation.

Second, a tissue-mimicking phantom (comprising "gelwax"; a mixture of mineral oil and glass microspheres with physiologically accurate ultrasound speckle [10]) emulating the vasculature of a human placenta was imaged. In this case, a wider aperture spanning 12.6 mm and comprising 128 equidistantly spaced sources was scanned, and 400-fold averaging was applied.

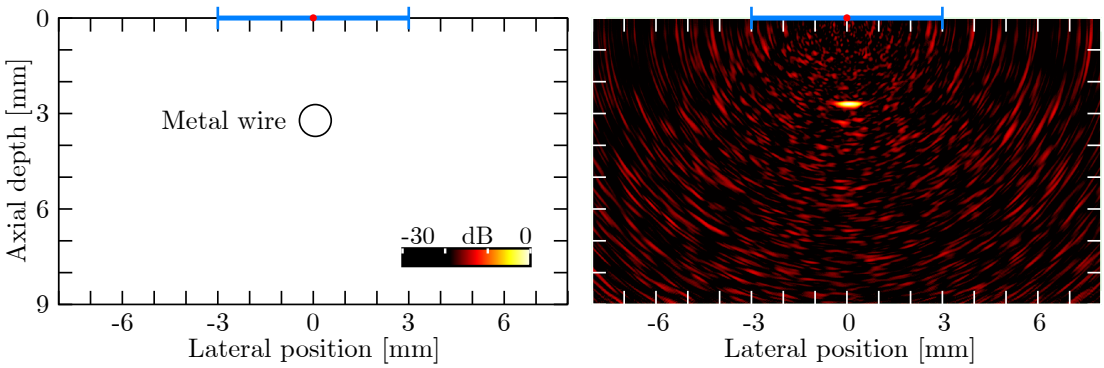

Fig. 2. Schematic (left) and NC-OpUS image (right) of a metal wire suspended in water. The blue line indicates the imaging aperture, the red dot the LDV interrogation location, and 64 source positions were distributed across the aperture.

In both scenarios, the phantom was submerged in water and the custom membrane was positioned at the air-water interface to emulate the skin. The LDV detection spot was placed centrally within the imaging aperture, but was elevationally offset by 1 mm. This was necessitated by the different optical requirements for the detection and generation of optical ultrasound, but also prevented surface waves propagating along the membrane from reducing LDV SNR.

III. Results

Non-contact optical ultrasound imaging of the wire target (Fig. 2) yielded a spatial resolution of 400 µm (lateral) by 150 µm (axial), and real-time acquisition, reconstruction and visualisation was achieved at a frame rate of 22 FPS. In this scenario, the NC-OpUS imaging system achieved a contrast-to-noise ratio (CNR) of 20.1 dB. This high frame rate was achieved through the combination of a narrow imaging aperture (requiring relatively low number of sources), a high echogenicity of the imaging target (thus requiring no signal averaging), and an omni-directional reflectivity of the imaging target (ensuring a high pulse-echo SNR across the aperture).

For the tissue-mimicking phantom (Fig. 3), the system achieved a CNR of 21.5 dB, but an image acquisition time of 26.7 s was required for this material exhibiting physiologically accurate contrast. This increased acquisition time was a result of a wider imaging aperture (comprising a twice the amount of sources), a lower echogenicity of the gelwax, and the specular nature of the pulse-echo signal off the phantom interface. This specular reflection resulted in significant deterioration in pulse-echo SNR with increasing lateral offset. The latter two effects necessitated 400-fold averaging to achieve a reasonable CNR.

IV. Discussion and Conclusion

This work is the first demonstration of a non-contact optical ultrasound imaging system capable of video-rate, real-time imaging. The system is compact and allows for a variable separation distance between object and imaging setup. Using metallic point targets, a frame rate of 22 Hz was achieved, which would be sufficient for, e.g., instrument or needle tracking applications – and would hence already offer clinical relevance.

For tissue-mimicking phantoms, significantly longer acquisition times of *ca.* 27 s per frame were required. This was due to a combination of a larger imaging aperture resulting in more source positions, and a lower NC-OpUS SNR necessitating significant averaging. However, this acquisition time can be significantly improved. Firstly, in future work the excitation laser will be exchanged with a model exhibiting 2.3-fold higher pulse energy, and the optics will be optimised to achieve tighter optical focussing. Combined, these two improvements are expected to achieve $5-10$ times higher NC-OpUS amplitudes, which could reduce the required number of averages by up to two orders of magnitude.

In addition, alternative SDA geometries will be employed to optimise imaging with apertures where the source separation distance exceeds the spatial Nyquist limit. Furthermore, the LDV beam path will be modified to achieve dynamic positioning of both the detector spot and the excitation spot. This will aid in further maximising the NC-OpUS SNR, as well as improve performance for specularly reflective objects.

Presently, the working distance between the NC-OpUS setup enclosure and the imaging target is approximately 28 cm. However, both the LDV detector and excitation laser allow for dynamic focussing to arbitrary distances, and the LDV is able to achieve a spot size below 125 µm, required to ensure omnidirectional sensitivity across the entire 12 MHz bandwidth, for distances of up to 1.5 m – thus enabling a wide range of working distances. This working distance can be further enhanced by allowing for weak detector directivity.

Finally, in this work, only fully-submerged phantoms were considered, where the NC-OpUS generating membrane was suspended at the air-water interface. However, this does not truly reflect the future clinical application. In future experiments, this membrane will be deposited onto the surface of tissue-mimicking phantoms and tissue samples directly. To this aim, a method of bonding these membranes to skin has been developed, allowing for strong and durable bonds (exceeding 1 hour wear time) in a matter of minutes. Importantly, these bonds are acoustically invisible. Full details are not included as intellectual property protection for this method is currently being pursued. However, additional research into the optical

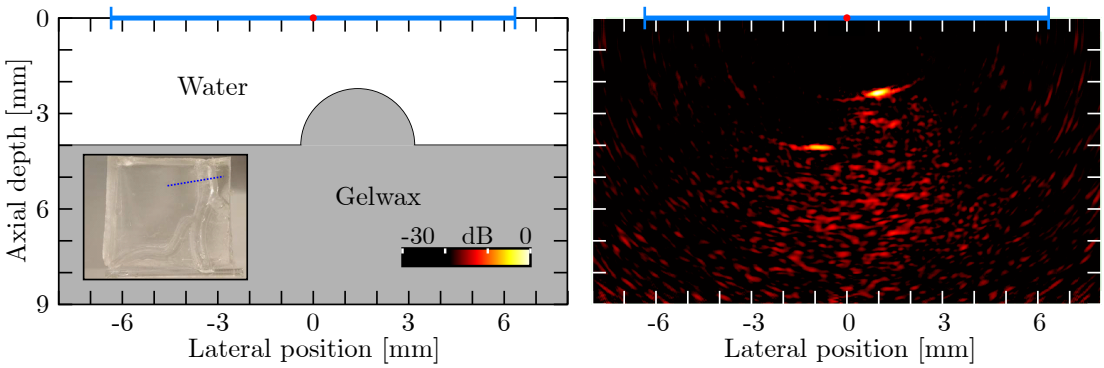

Fig. 3. Schematic (left) and NC-OpUS image (right) of a tissue-mimicking phantom comprising gelwax suspended in water. The blue line indicates the imaging aperture, the red dot the LDV interrogation location, and 128 source positions were distributed across the aperture. The inset shows a photograph of the phantom and indication of the imaging aperture (dashed line).

and thermal safety, as well as the imaging performance in case of curved or even moving surfaces, will need to be performed before human imaging can be attempted.

This proceeding presents important progress towards real-time, dynamic, biomedical non-contact optical ultrasound imaging at frame rates suitable for clinical applications. The system currently has clinical relevance for highly echogenic objects such as metal targets (e.g. needles, fiducial markers, surgical instrument tracking), and a realistic path towards achieving sub-second acquisition times for tissue mimicking phantoms and actual tissue samples is presented. As such, the presented system shows great potential for future clinical use, where it will enable ultrasound imaging in crowded surgical settings, facilitate intra-operative imaging by reducing the risk of infection or contact trauma, and allow for hands-free imaging during surgical treatment.

REFERENCES

[1] Richard S C Cobbold. *Foundations of Biomedical Ultrasound*. Oxford University Press, USA, New York, 2007.

[2] Masoud Shaloo, Martin Schnall, Thomas Klein, Norbert Huber, and Bernhard Reitinger. A review of non-destructive testing (ndt) techniques for defect detection: Application to fusion welding and future wire arc additive manufacturing processes. *Materials*, 15(10):3697, 2022.

[3] Jami L Johnson, Jeffrey Shragge, and Kasper van Wijk. Nonconfocal all-optical laser-ultrasound and photoacoustic imaging system for angle-dependent deep tissue imaging. *Journal of Biomedical Optics*, 22(4):041014–041014, 2017.

[4] Xiang Zhang, Jonathan R Fincke, Charles M Wynn, Matt R Johnson, Robert W Haupt, and Brian W Anthony. Full noncontact laser ultrasound: First human data. *Light: Science & Applications*, 8(1):1–11, 2019.

[5] Jakub Spytek, Lukasz Ambrozinski, and Ivan Pelivanov. Non-contact detection of ultrasound with light–review of recent progress. *Photoacoustics*, page 100440, 2022.

[6] Erwin J Alles and Adrien E Desjardins. Source density apodisation: Image artefact suppression through source pitch non-uniformity. *IEEE transactions on ultrasonics, ferroelectrics, and frequency control*, 2019.

[7] Jørgen Arendt Jensen, Svetoslav Ivanov Nikolov, Kim Løkke Gammelmark, and Morten Høgholm Pedersen. Synthetic aperture ultrasound imaging. *Ultrasonics*, 44:e5–e15, 2006.

[8] Semyon Bodian, Esra Aytac-Kipergil, Shaoyan Zhang, et al. Comparison of fabrication methods for fiber-optic ultrasound transmitters using candle-soot nanoparticles. *Advanced Materials Interfaces*, 10(9):2201792, 2023.

[9] Sacha Noimark, Richard J Colchester, Ben J. Blackburn, et al. Carbon-nanotube-PDMS composite coatings on optical fibres for all-optical ultrasound imaging. *Advanced Functional Materials*, 26(35), 2016.

[10] Efthymios Maneas, Wenfeng Xia, Daniil I Nikitichev, et al. Anatomically realistic ultrasound phantoms using gel wax with 3D printed moulds. *Physics in Medicine & Biology*, 63(1), 2018.